Colloids

DOI: 10.1002/anie.200804704

Schooling Behavior of Light-Powered Autonomous Micromotors in Water**

*Michael Ibele, Thomas E. Mallouk, and Ayusman Sen**

One of the great scientific challenges is the creation of nano- or microscale machines that can function collectively to accomplish tasks such as chemical sensing, particle assembly, and drug delivery. These tasks require communication and cooperation between individual machines. While advances have been made in the fabrication of autonomous nano- and micromotors,[1–10] there have been no reports of cooperative behavior between such motors. In the biological world, collective behavior is quite common. For instance, the unicellular slime mold amoebae *Dictyostelium discoideum* will secrete a signaling chemical into the environment when stressed. Nearby slime molds will then move up the chemical gradient and assemble to form a multicellular fruiting body.[11–14] We report herein that micrometer-sized silver chloride (AgCl) particles move under UV illumination in deionized water by self-diffusiophoresis. Like the *Dictyostelium discoideum*, each AgCl particle secretes chemicals (ions) as it moves, to which the other particles respond by "schooling" into regions with higher particle concentrations. When photo-inactive silica particles are mixed with the AgCl, the latter respond to the ion secretion by swimming towards and surrounding individual AgCl particles. Our system can be used as a nonbiological model for intercellular communication.[14,15] More importantly, it demonstrates new design principles for "intelligent" synthetic nano or micromachines that function collectively. For example, the "predator–prey"-like behavior of the AgCl/silica particle system illustrates how two different particle types can move autonomously in order to organize themselves spatially.

AgCl particles (ca. 1 μm in diameter) in deionized water move autonomously at speeds of up to 100 $\mu m s^{-1}$ when exposed to ultraviolet (UV) light (Figure 1; see also Video 1 in the Supporting Information). This autonomous motion is due to the asymmetric photodecomposition of the particles. The asymmetry in the decomposition rate is likely due to either particle surface heterogeneity or nonuniform photoexposure of the particle. The asymmetric photodecomposition creates a localized electrolyte gradient around the particle to result in self-diffusiophoresis that is analogous to the diffusiophoretic movement of particles in an externally imposed electrolyte gradient.[16]

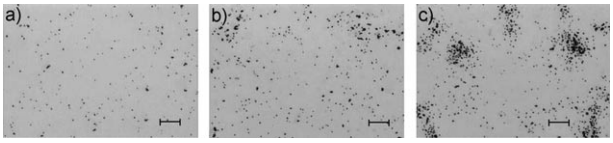

Figure 1. AgCl particles in deionized water a) before UV illumination, b) after 30 s of UV exposure, and c) after 90 s (see Video 1 in the Supporting Information). Images are read left to right. Scale bars: 20 μm.

The motion of the AgCl particles can be made more directional by the addition of an inert rudder. When amidine-functionalized polystyrene microspheres (AFP-spheres, 2.3 μm; $\zeta_P = +40$ mV, where ζ_P is the zeta potential of any colloid in the system for which the speed (U) is being calculated [see also Eq. (2)]) are present in the UV-illuminated AgCl particle solution, the AFP-spheres become caught in the local ion gradient around the individual AgCl particles. As a result, they are diffusiophoretically pumped towards the AgCl, where they become electrostatically attached to the AgCl particles ($\zeta_P = -52$ mV). The resulting Janus particles have a much higher degree of asymmetry and, as expected, a much more linear trajectory (see Video 2 in the Supporting Information). If silica particles (2.14 μm; $\zeta_P = -49$ mV) are used instead of AFP-spheres, the silica particles surround the AgCl but do not attach because of their negative zeta potential (see Video 3 in the Supporting Information).

Because the AgCl particles are both the source of the electrolyte gradient and are translated by it, interesting ensemble patterning phenomena emerge. After 1–5 minutes, mesoscale "schools" of AgCl particles are observed (Figure 1 a–c and Video 1 in the Supporting Information). These schools are quite stable and rarely, if ever, lose member particles back into the bulk solution. A similar clustering behavior in response to the secreted chemicals of individuals is seen in some quorum-sensing unicellular organisms.[11–14]

In a typical experiment, 50 μL of deionized water containing AgCl particles was placed in a round well on a microscope slide (Figure 1). UV light (320–380 nm, 2.5 $W cm^{-2}$) was focused onto the particles through the microscope objective from below. Since AgCl particles are rather dense (5.56 $g cm^{-3}$), they settle to within a few micrometers above the glass slide surface. Electrostatic repulsion keeps the particles from coming directly into contact with the slide surface. For imaging purposes, the sample was backlit with low-intensity (6 $mW cm^{-2}$) broad-band visible-wave-

[*] M. Ibele, Dr. T. E. Mallouk, Dr. A. Sen
Department of Chemistry, The Pennsylvania State University
University Park, PA 16802 (USA)
Fax: (+1) 814-865-1543
E-mail: asen@psu.edu
Homepage: http://research.chem.psu.edu/axsgroup/

[**] We thank Penn State Center for Nanoscale Science (NSF-MRSEC, DMR-0213623, and DMR-0820404) for financial support and Drs. Vincent Crespi and Darrell Velegol for helpful discussions.

Supporting information for this article is available on the WWW under http://dx.doi.org/10.1002/anie.200804704.

length light from above. This low-intensity visible-wavelength light had no observable effect on fresh samples of AgCl (see below).

Although the photosensitive properties of AgCl are well known and have been exploited in black and white photography since the mid-19th century, only recently has the exact mechanism of the UV-induced dissolution of AgCl been elucidated.[17] The overall reaction at pH 5 is shown in Equation (1).

$$4\,AgCl + 2\,H_2O \xrightarrow{h\nu,\ Ag^+} 4\,Ag + 4\,H^+ + 4\,Cl^- + O_2 \quad (1)$$

The electrolyte gradient that powers the motion of the AgCl particles is created by the production of protons and chloride ions in solution. The plating out of silver metal onto the particles causes their speed to decay such that, after 30 minutes, there is no visible non-Brownian motion, and the particles are black in color.[18]

Unlike other bubble-powered micromotors,[6,19,20] no oxygen bubbles are seen in this system because of the relatively show reaction rate. The mechanism of particle motion and organization is not optical trapping, since the phenomenon was not observed for photo-insensitive colloids. A map of the UV light intensity produced by our microscope was roughly Gaussian in nature and contained no "hot spots". If such a beam resulted in optical trapping, particles would be shuttled to the beam center and would not form dozens of isolated "schools".

Diffusiophoresis is the motion of particles that arises from an electrolyte gradient. The diffusiophoretic speed of particles near a wall in a monovalent salt gradient can be approximated by using Equation (2),[16] where U is the

$$U = \underbrace{\left(\frac{dLn(C)}{dx}\right)\left(\frac{D_C - D_A}{D_C + D_A}\right)\left(\frac{k_B T}{e}\right)}_{\text{Electric Field}} \frac{\varepsilon(\zeta_P - \zeta_W)}{\eta} + \left(\frac{dLn(C)}{dx}\right)\left(\frac{2\varepsilon k_b^2 T^2}{\eta e^2}\right) Ln\left[1 - \tanh\left(\frac{e\zeta_W}{4k_b T}\right)^2\right] \quad (2)$$

particle speed, $dLn(C)/dx$ is the electrolyte gradient, D_C and D_A are the diffusion constants of the cation and anion components of the gradient, k_B is the Boltzmann constant, T is the temperature, e is the elementary charge, ε is the solution permittivity, η is the dynamic viscosity of the solution, ζ_P is the zeta potential of the particle, and ζ_W is the zeta potential of the wall (glass slide). The motion described by Equation (2) results from the fact that cations and anions contributing to the ion gradient in a given direction diffuse at different rates. This difference results in a net electric field in solution that acts both phoretically on particles in solution and osmotically on any nearby wall double layer. Additionally, since the thickness of the ionic double layer on the wall depends strongly on the electrolyte concentration in solution, an electrolyte gradient will result in a gradient in double-layer thickness along the wall. This gradient in double-layer thickness creates an effective "pressure" difference along the wall, represented by the second term in Equation (2), which causes fluid to flow from the area of higher electrolyte concentration to the area of lower concentration.

We first considered how Equation (2) relates to the diffusiophoretic interaction between an AgCl particle and a positively charged AFP-sphere. As the AgCl decomposes into protons and chloride ions, the protons travel away from the surface of the AgCl much faster than the chloride ions ($D_{H^+} = 9.311 \times 10^{-5}\ cm^2\,s^{-1}$, $D_{Cl^-} = 1.385 \times 10^{-5}\ cm^2\,s^{-1}$). The different diffusion rates result in a net electric field in solution, and, in the case of the AgCl, the electric field points back towards the AgCl particle. This electric field acts phoretically on the positively charged AFP-sphere by pulling it towards the AgCl. The electric field also acts osmotically on the adsorbed protons in the double layer of the microscope slide wall ($\zeta_W = -62$ mV[21]) by pumping the fluid along the slide's surface towards the AgCl particles. The double-layer thickness pressure term counteracts this slightly, and attempts to pump the fluid away from the AgCl. Thus, from Equation (1), positive ζ_P and negative ζ_W values in the first term work in concert and are large enough to overcome the contribution from the double-layer pressure; this results in the AFP-sphere sticking to the photodecomposing AgCl particle. The resulting AgCl/AFP Janus particles are highly asymmetric, and, as a result, have significantly better linear trajectories.

Let us now consider the interaction between one AgCl particle and a tracer particle with a ζ_P value of approximately -50 mV (a "passive" AgCl particle or a silica particle). Again the electroosmotic flow direction along the slide's surface is towards the AgCl, and the pressure flow direction is outwards. However, in this case, the electrophoretic force direction of the tracer particle is away from the AgCl. Because the magnitude of the particle zeta potential is less than that of the slide, the osmotic flow dominates, and is sufficient to still overcome both the double-layer pressure term and the phoretic motion of the particles. The dominance is valid as long as both particles are in the same plane along the wall's surface. However, because the fluid along the slide's surface is osmotically pumped inward towards the AgCl from all directions, fluid continuity dictates that the osmotic flow in the plane of the slide approaches zero very near to the AgCl as the fluid is forced upwards and away from the slide surface. Therefore, the outward phoretic force on the tracer particle dominates very near the AgCl particle. Thus, the particles will be pumped towards one another to form schools, but will not stick together and form clumps.

In fact, this behavior is exactly what is observed when 2.1 μm silica particles (ζ_P, -49 mV) were added to a dilute solution of AgCl particles ($\zeta_P = -52$ mV). While the UV light is on, silica particles actively seek out the mobile AgCl particles and surround them, while still maintaining a small exclusion zone (ca. 2–3 μm) around the AgCl particle. When the UV light is turned off, this exclusion zone disappears (Figure 2 and Video 3 in the Supporting Information). Thus, the procedure provides a facile energy-efficient method of spatially arranging different particle types.

The way in which an individual AgCl particle swims is not much different to the behavior outlined above. The asymmetric photodecomposition of an individual AgCl particle creates a net increase in ion concentration on one side of the particle. The entire particle then responds diffusiophoretically

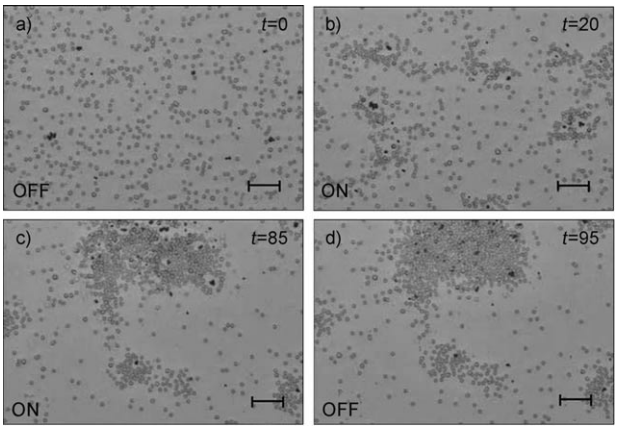

Figure 2. "Predator–prey" behavior of two different particles. AgCl particles (darker objects) were mixed with 2.34 μm silica spheres and placed in deionized water (a). When illuminated with UV light (b, c) the silica spheres actively seek out the AgCl particles and surround them. While the UV light is on, an exclusion zone is seen around the AgCl particles; this exclusion zone disappears when the UV light is turned off (d). Times (t; seconds) are given in the upper right corner. The status of the UV light is given in the bottom left corner. Scale bars: 20 μm.

to this ion gradient, which is continuously reestablished in the presence of UV light.

The schooling behavior of these AgCl particles is different from the more common phenomenon of Ostwald ripening, which is a thermodynamically driven, passive process of aggregation in which smaller particles combine to reduce their total surface area. Upon illumination, the AgCl particles actively organize into higher-density regions while still maintaining a finite particle spacing. Since there is no reduction of particle surface area, Ostwald ripening is not the mechanism that occurs in our system. A control experiment showed that solutions of non-illuminated particles did not school into higher-density regions, although they should still undergo Ostwald ripening if it were the dominant mechanism.

The relative magnitude of the gradient can be controlled by adjusting the concentration of ions in the bulk solution (C_{bulk}). Indeed, in accordance with Equation (3), a linear plot

$$\frac{dLn(C)}{dx} \approx \frac{\Delta Ln(C)}{\Delta x} = \frac{\Delta C}{C\Delta x} = \frac{(C_{bulk} + C_{rxn}) - (C_{bulk})}{C_{bulk}\Delta x} = \frac{C_{rxn}}{C_{bulk}\Delta x} \qquad (3)$$

of particle speed versus $1/C_{bulk}$ was obtained when varying amounts of KNO_3 (an unreactive salt) were added to the solution, thus supporting the proposed diffusiophoretic mechanism (Figure 3).

As noted above, the direction of the electric field that induces the diffusiophoretic flow is dictated by the relative mobilities of the constituent ions of the electrolyte. In the AgCl system, the cations (protons) are faster than the anions (chloride ions). As such, it would be expected that the pumping direction would be reversed in systems where the relative mobilities are reversed. To test this hypothesis, 2.1 μm silica particles were mixed with magnesium oxide microrods (ca. 75 μm long). In water, MgO forms the relatively insoluble

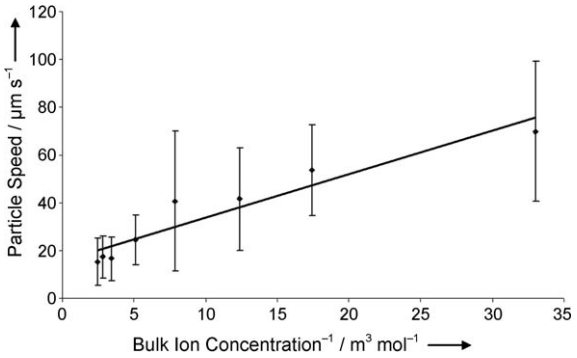

Figure 3. Speed of the AgCl particles during the first two seconds of UV illumination plotted versus the inverse of the concentration KNO_3 in the bulk solution (extrapolated from the bulk conductivity[9]). Error bars are one standard deviation. Each point represents thirty particles tracked.

magnesium hydroxide $Mg(OH)_2$ ($K_{sp} = 1.6 \times 10^{-12}$). The low solubility of $Mg(OH)_2$ ensures low bulk ion concentration that allows higher diffusiophoretic rates [see Eq. (3)]. Furthermore, the mobility of the cation (Mg^{2+}) is lower than that of the anion (OH^-) ($D_{Mg^{2+}} = 0.706 \times 10^{-5}\ cm^2 s^{-1}$, $D_{OH^-} = 5.273 \times 10^{-5}\ cm^2 s^{-1}$). As expected, the silica particles along the surface of the microscope slide were pumped outward from the MgO microrods by the electroosmotic flow (Figure 4). Meanwhile, silica particles that settling from the

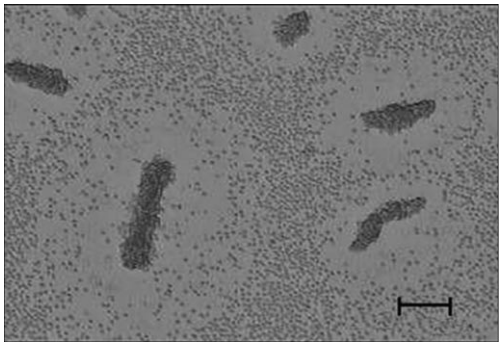

Figure 4. MgO microrods (large objects) in deionized water containing 2.14 μm silica particles. An exclusion zone is seen around each MgO microrod. The MgO microrods are also coated with silica tracers, which have settled down from the bulk solution. Scale bar: 50 μm.

bulk solution near the MgO are attracted to the MgO microrods because of the electrophoretic attraction between the two particles. Thus, in both the AgCl/silica and the $Mg(OH)_2$/silica systems, the electroosmotic flow dominates for particles along the microscope slide surface, except for the region directly adjacent to the ion-producing particle, and, as expected, the direction of this osmotic pumping is opposite for the two systems. The electrophoretic force on the tracers dominates very near the ion-producing particle, because of fluid continuity and the direction of the electrophoretic force, which again is opposite in the two systems. Thus, our observations strongly support the proposed diffusiophoretic mechanism.

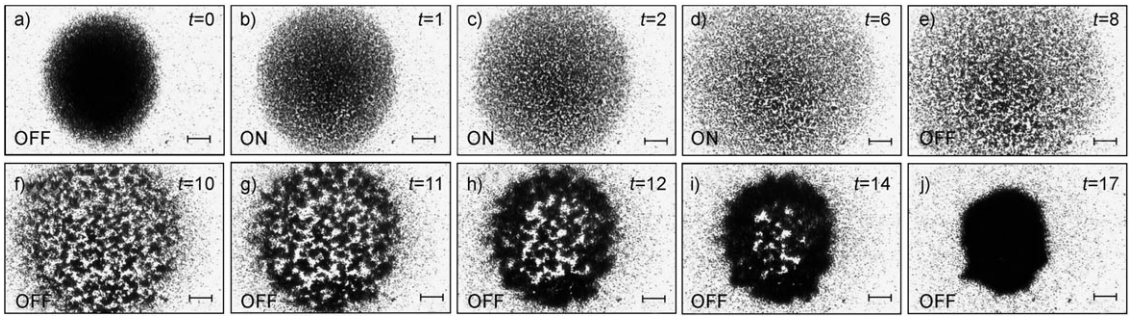

Figure 5. A large school of AgCl particles previously exposed to UV light are observed under visible light (a). The UV light is turned back on directly after image (a) and the interparticle spacing expands. The UV light is turned off again directly after image (d) and the interparticle spacing diminishes again (see Video 4 in the Supporting Information). Times (t; seconds) are given in the upper right corner. The status of the UV light is given in the lower left corner. Scale bars: 20 μm.

An additional interesting effect was observed when an assembly of AgCl particles previously exposed to UV light was placed in purely visible light (Figure 5 a–j and Video 4 in the Supporting Information). In this experiment, AgCl particles were initially illuminated with UV light from the microscope objective below and low intensity visible light from above, and, as noted above, the particles created mesoscale schools with interparticle spacings on the order of 1–2 μm. After some time (ca. 10 min), the UV light was turned off, leaving only the visible-wavelength backlighting. This procedure resulted in a tighter school. Switching the UV light source back on resulted in the re-expansion of the interparticle spacing to their original values. This procedure could be repeated over many cycles, with the interparticle spacing of the school of particles being increased by the combination of UV and visible light, and then being reduced by purely visible light. It should be noted that the reduction of the particle spacing with visible light was only observed with particles previously exposed to UV light. Fresh AgCl particles showed no response to the low-intensity visible light. Our tentative hypothesis for this behavior is as follows. When the UV light is turned off, the individual particles no longer secrete ions as dictated by Equation (1), thus the local ion gradients that surround the individual particles dissipate. As a result, the phoretic repulsive force between individual particles decreases, which allows the AgCl to pack tighter while the UV light is off—assuming there is still an attractive force that brings the particles together. The origin of this attractive force remains unclear. Considering the fast diffusion rate of the ions, it is unlikely that any ion gradient produced by the UV reaction would remain in place long enough to result in this attraction. One possible explanation is a second, visible-light-initiated chemical reaction by the AgCl, that is, a reaction that occurs only after the particles have been exposed to wavelengths in the UV region. Indeed, AgCl is known to "self-sensitize" in water, a process in which the silver metal created by the reaction with UV light [see Eq. (1)] alters the surface chemistry of AgCl, thus making it sensitive to visible light.[17]

In conclusion, we have described the simplest autonomous micromotor reported to date. The only "fuel" needed to induce motion is UV light. In addition, the AgCl micromotors can self-assemble with passive objects and thereby alter their trajectory. Finally, solutions that contain a high concentration of AgCl micromotors exhibit collective behavior similar to that shown by quorum-sensing single cell organisms. Thus, our motors serve as a nonbiological model for the study of cell signalling and collective, emergent, behavior.[14,15] More importantly, it demonstrates new design principles for "intelligent" synthetic nano or micromachines that function collectively. There are many possible ways of designing ion-producing nano- or microparticles, including particles with attached catalysts or enzymes that form ions as products. Furthermore, these particles should interact with each other or with inert nano- or microparticles. In addition, the design principle allows the coordinated movement of dissimilar particles that are not attached to each other making it easier to transport and deliver cargo at designated areas.

Experimental Section

In a typical experiment, 50 μL of a solution of AgCl particles in deionized water was placed inside a circular well (9 mm diameter, 0.12 mm deep, Secure Seal Spacer, Invitrogen) on a microscope slide and imaged with a microscope (Zeiss, Axiovert 200 Mat). UV light (320–380 nm, 2.5 W cm^{-2}, Chroma 31000v2) was provided through the 50× imaging objective, resulting in a spot size of approximately 0.6 mm. UV light intensity was measured with a UV Light Meter (Mannix). Visible light intensity was measured with a 1935T-C Power Meter (Newport)

Particle trajectories were tracked manually using PhysVis (Kenyon College). Zeta potentials were measured in the absence of light with a ZetaPALS instrument.

See the Supporting Information for details of particle synthesis.

Received: September 25, 2008
Revised: February 20, 2009
Published online: March 31, 2009

Keywords: colloids · diffusiophoresis · photochemistry · self-assembly · silver

[1] a) W. Paxton, S. Sundararajan, T. Mallouk, A. Sen, *Angew. Chem.* **2006**, *118*, 5546–5556; *Angew. Chem. Int. Ed.* **2006**, *45*, 5420–5429; b) J. Wang, *ACS Nano* **2009**, *3*, 4–9.

[2] a) W. Paxton, K. Kistler, C. Olmeda, A. Sen, S. St. Angelo, Y. Cao, T. Mallouk, P. Lammert, V. Crespi, *J. Am. Chem. Soc.* **2004**,

126, 13424 – 13431; b) W. Paxton, P. Baker, T. Kline, Y. Wang, T. Mallouk, A. Sen, *J. Am. Chem. Soc.* **2006**, *128*, 14881 – 14888.
[3] S. Fournier-Bidoz, A. Arsenault, I. Manners, G. Ozin, *Chem. Commun.* **2005**, 441 – 443.
[4] J. Howse, R. Jones, A. Ryan, T. Gough, R. Vafabakhsh, R. Golestanian, *Phys. Rev. Lett.* **2007**, *99*, 048102.
[5] T. Kline, W. Paxton, T. Mallouk, A. Sen, *Angew. Chem.* **2005**, *117*, 754 – 756; *Angew. Chem. Int. Ed.* **2005**, *44*, 744 – 746.
[6] J. Vicario, R. Eelkema, W. Browne, A. Meetsma, R. La Crois, B. Feringa, *Chem. Commun.* **2005**, 3936 – 3938.
[7] M. Ibele, Y. Wang, T. Kline, T. Mallouk, A. Sen, *J. Am. Chem. Soc.* **2007**, *129*, 7762 – 7763.
[8] S. Sundararajan, P. Lammert, A. Zundans, V. Crespi, A. Sen, *Nano Lett.* **2008**, *8*, 1271 – 1276.
[9] T. Kline, A. Sen, *Langmuir* **2006**, *22*, 7124 – 7127.
[10] Y. Hong, N. Blackman, N. Kopp, A. Sen, D. Velegol, *Phys. Rev. Lett.* **2007**, *99*, 178103.
[11] P. Devreotes, *Science* **1989**, *245*, 1054 – 1058.
[12] L. Eichinger, et al., *Nature* **2005**, *435*, 43 – 57.
[13] K. Jarrell, M. McBride, *Nat. Rev. Microbiol.* **2008**, *6*, 466 – 476.
[14] U. Wilensky, NetLogo Slime model, http://ccl.northwestern.edu/netlogo/models/Slime, Center for Connected Learning and Computer-Based Modeling, Northwestern University, Evanston, IL, **1997**.
[15] A. Goldbeter, *Math. Biol.* **2006**, *68*, 1095 – 1109.
[16] J. Anderson, *Annu. Rev. Fluid Mech.* **1989**, *21*, 61 – 99.
[17] G. Calzaferri, *Catal. Today* **1997**, *39*, 145 – 157.
[18] See the Supporting Information for FESEM images.
[19] J. Kao, X. Wang, J. Warren, J. Xu, D. Attinger, *J. Micromech. Microeng.* **2007**, *17*, 2454 – 2460.
[20] Y. Mei, G. Huang, A. Solovev, E. Urena, I. Monch, F. Ding, T. Reindl, R. Fu, P. Chu, O. Schmidt, *Adv. Mater.* **2008**, *20*, 4085 – 4090.
[21] Y. Gu, D. Li, *J. Colloid Interface Sci.* **2000**, *226*, 328 – 339.

